OPEN

Discovery of Novel *TULP4/ACTN4/EWSR1/ACTB::MYB* and *ESRRG::DNM3* Fusions Expands Molecular Landscape of Adenoid Cystic Carcinoma Beyond Fusions Between *MYB/MYBL1* and *NFIB* Genes

Alena Skálová, MD, PhD,† Natálie Klubíčková, MD, PhD,*† Martina Bradová, MD, PhD,*† Abbas Agaimy, MD,‡ Niels J. Rupp, MD, PhD,§ Ivan Damjanov, MD, PhD,‖ Georgina Kolnikova, MD,¶ Petr Martínek, PhD,# Petr Šteiner, PhD,# Petr Grossmann, PhD,# Tomas Vaněček, PhD,# Michal Michal, MD,*† and Ilmo Leivo, MD, PhD***

Abstract: Adenoid cystic carcinoma (AdCC) is one of the most common salivary gland malignancies and occurs in all major and minor salivary gland and seromucous gland sites. AdCCs of salivary gland origin have long been categorized as fusion-defined carcinomas owing to the almost consistent presence of fusion genes *MYB::NFIB,* or less commonly *MYBL1::NFIB.* We collected a cohort of 95 cases of AdCC, which were largely characterized by canonical fusions *MYB::NFIB* (49 cases) or *MYBL1::NFIB* (9 cases). In additional 11 cases of AdCC, rearrangements in *MYB* or *NFIB* genes were detected by FISH. In addition, NGS revealed novel noncanonical fusion transcripts *EWSR1::MYB*; *ACTB::MYB; ESRRG::DNM3, MYB::TULP4*, and *ACTN4::MYB*, each of them in 1 case. The tumors that showed noncanonical fusions had features of metatypical AdCC with a diverse architecture, lobulated multinodular growth pattern, and hypercellular peripheral palisading of nuclei (2 cases), tubular hypereosinophilia (2 cases), and pale eosinophilic to vacuolated (bubbly) cytoplasm (3 cases). Our study documented 3 cases of AdCC of salivary glands harboring novel gene fusions *TULP4::MYB*, *ACTN4::MYB,* and *ACTB::MYB*, in 1 case each, which have not been described before. A rare *EWSR1::MYB* fusion was detected in 1 case. Moreover, 1 case of sinonasal metatypical AdCC showed *EWSR1* rearrangement detected by FISH. Also, 1 case with an *ESRRG::DNM3* fusion of unknown significance is described in this study. These discoveries illustrate how broad molecular profiling will expand understanding of changes in known entities.

Key Words: salivary gland neoplasm, sinonasal, adenoid cystic carcinoma, *TULP4/ACTN4/EWSR1/ACTB::MYB* gene fusion, novel *ESRRG::DNM3* gene fusion

(*Am J Surg Pathol* 2024;00:000–000)

Salivary gland tumors represent one of the most challenging areas in diagnostic head and neck pathology. These rare tumors exhibit a diverse array of morphologic features, comprising over 30 subtypes in the current World Health Organization (WHO) classification of head and neck tumors.[1] Over the past decade, there have been significant developments in genomic medicine and our understanding of the genomic landscape of human tumors, including salivary gland neoplasms.[2] Tumor type–specific gene fusions have been described in various salivary gland tumors in recent years, and a predominant canonical

From the *Department of Pathology, Faculty of Medicine in Pilsen, Charles University, Czech Republic; †Bioptic Laboratory, Ltd., Pilsen, Czech Republic; #Molecular and Genetic Laboratory, Bioptic Laboratory, Ltd, Pilsen, Czech Republic; ‡Institute of Pathology, University Hospital Erlangen, Friedrich-Alexander University Erlangen-Nürnberg (FAU), Erlangen, Germany; §Department of Pathology, and Molecular Pathology, University Hospital Zurich, Zurich, Switzerland; ‖The University of Kansas School of Medicine, Kansas City, KS; ¶Department of Pathology, National Oncologic Institute, Bratislava, Slovak Republic; and **Institute of Biomedicine, Pathology, University of Turku and Department of Pathology, Turku University Hospital, Turku, Finland.

The preliminary results of the study were presented as a poster presentation at the United States and Canadian Academy of Pathology's 113th Annual Meeting, March 23–28, 2024, in Baltimore, MD.

This study was supported by study grant SVV 260652 from the Ministry of Education of the Czech Republic (N.K.), the Cooperation Program—research area SURG from the Charles University, Czech Republic (N.K., M.B., and A.S.), the project National Institute for Cancer Research—NICR (Programme EXCELES, ID Project No. LX22NPO5102)—Funded by the European Union—Next Generation EU (A.S. and M.B.), and Turku University Hospital Fund, Maritza and Reino Salonen Foundation, and the Finnish Cancer Society, Finland (I.L.).

Conflicts of Interest and Source of Funding: The authors have disclosed that they have no significant relationships with, or financial interest in, any commercial companies pertaining to this article.

Correspondence: Alena Skálová, MD, PhD, Sikl's Department of Pathology, Faculty of Medicine in Pilsen, Charles University, E. Benese 13, Pilsen 305 99, Czech Republic (e-mail: skalova@biopticka.cz).

DOI: 10.1097/PAS.0000000000002304

fusion is detected in a large proportion of cases in a given tumor entity.[3] In addition, alternative gene partners have been found in a minority of cases of such entities.[4–6]

Adenoid cystic carcinomas (AdCC) of salivary gland origin have long been categorized as fusion-defined carcinomas owing to the nearly consistent presence of the fusion genes *MYB::NFIB* or *MYBL1::NFIB*.[7,8] Since then, further exploration has unveiled additional partner genes linked to *MYB* and *NFIB* such as *EWSR1::MYB*, *FUS::MYB*[9] and *MYB::PDCD1LG2*, *MYB::EFR3A*, and *NFIB::AIG1*,[10] enriching our understanding of these entities. Intriguingly, a subset of AdCCs lacks these rearrangements, raising questions about possible additional fusion-transcript mechanisms. Such a lack of molecular understanding is especially troublesome when dealing with small biopsy samples where AdCC could be mistaken for other entities.

In our current study of 95 sinonasal and salivary AdCCs, we have documented 4 cases that display novel fusions with alternative partners for the *MYB* gene, such as *TULP4*, *ACTN4, EWSR1,* and *ACTB* in 1 case each. One case of this cohort harbored the *EWSR1::MYB* transcript, which has been preliminarily reported previously.[9] Moreover, one of our cases of metatypical AdCC in a sinonasal location harbored a completely novel noncanonical gene fusion *ESRRG::DNM3*.

Elucidation of these molecular intricacies may hold the key to understanding the pathogenesis and clinical behavior of such carcinomas, paving the way for improved diagnostic and therapeutic approaches.

MATERIALS AND METHODS

Case Selection

The cases were retrieved from the consultation files of the Tumor Registry at the Department of Pathology, Faculty of Medicine in Pilsen and Bioptic Laboratory, Ltd in Pilsen, Czech Republic, and the tumor registries of the co-authors. The tumors were examined histologically, immunohistochemically, by next-generation sequencing (NGS) and/or fluorescence in situ hybridization (FISH) looking for *MYB*/*MYBL1* and/or *NFIB* gene fusions or any novel gene fusions/mutations.

This study was approved by the Ethics Committee of the Faculty Hospital in Pilsen and Charles University, Faculty of Medicine in Pilsen, Czech Republic, on August 2, 2018.

Histologic and Immunohistochemical Studies

For conventional microscopy, the excised tissues were fixed in formalin, processed routinely, embedded in paraffin (FFPE), cut, and stained with hematoxylin and eosin.

For immunohistochemistry, 4-µm-thick sections were cut from paraffin blocks and mounted on positively charged slides (TOMO, Matsunami Glass IND). Sections were processed on a BenchMark ULTRA (Ventana Medical Systems), deparaffinized, and subjected to heat-induced epitope retrieval by immersion in a CC1 solution (pH 8.6) at 95°C. All primary antibodies used in this study are summarized in Table 1.

Visualization was performed using the ultraView Universal DAB Detection Kit (Roche) and ultraView Universal Alkaline Phosphatase Red Detection Kit (Roche). The slides were counterstained with Mayer's hematoxylin. Appropriate positive and negative controls were employed.

Molecular Studies

TruSight Oncology 500 Kit (TS500)

Mutation analysis and fusion transcripts detection were performed using TruSight Oncology 500 Kit (Illumina). RNA was extracted using the Maxwell RSC DNA FFPE Kit and the Maxwell RSC Instrument (Promega) according to the manufacturer's instructions and quantified using the Qubit HS RNA Assay Kit (Thermo Fisher Scientific). DNA was extracted using the QIAsymphony DSP DNA mini (Qiagen) and quantified using the Qubit BR DNA Assay Kit (Thermo Fisher Scientific). The quality of DNA was assessed using the FFPE QC kit (Illumina), and the quality of RNA was assessed using Agilent RNA ScreenTape Assay (Agilent). DNA samples with Cq < 5 and RNA samples with DV200 ≥ 20 were used for further analysis. After DNA enzymatic fragmentation with KAPAFrag Kit (KAPA Biosystems), DNA and RNA libraries were prepared with the TruSight Oncology 500 Kit (Illumina) according to the manufacturer's protocol. Sequencing was performed on the NovaSeq 6000 sequencer (Illumina) following the manufacturer´s recommendations. Data analysis was performed using the TruSight Oncology 500 v2.2 Local App (Illumina). Variant annotation and filtering were performed using the Omnomics NGS analysis software (Euformatics). A custom variant filter was set up

TABLE 1. Antibodies Used for Immunohistochemical Study

Antibody specificity	Clone	Dilution	Antigen retrieval/time	Source
AE1/3	AE1/AE3+PCK26	RTU	EnVision High pH /30 min	Dako
CK7	OV-TL 12/30	RTU	EnVision High pH/30 min	Dako
CK14	SP53	1:800	EnVision High pH/30 min	Cell Marque
p63	DAK-p63	RTU	EnVision Low pH/30 min	Dako
p40	DAK-p40	RTU	EnVision Low pH/30 min	Dako
SOX10	SP267	RTU	CC1/64 min	Cell Marque
Ki-67	MIlB-1	RTU	EnVision Low pH/30 min	Dako
MYB	EP769Y	1:100	CC1/64 min	AbCam

CC1 indicates EDTA buffer pH 8.6 at 95°C; EnVision High pH 9.0 at 97°C; EnVision Low pH 6.0 at 97°C; min, minutes; RTU, ready to use.

TABLE 2. Clinicopathological and Molecular Features of 5 Cases AdCC With Noncanonical Fusions

No.	Age/sex	Site	Original diagnosis	Treatment	Clinical course (mo)	Outcome/follow-up (mo)	Molecular-genetic analysis
1	55/M	Right maxillary sinus	Basal cell carcinoma	Surgery + radiotherapy	Recurrence (12)	DOD (72)	*ESRRG::DNM3*, *EWSR1* break-apart (FISH)
2	87/F	Parotid gland	Basal cell adenoma	diagnostic biopsy	Residual disease	AWD (6)	*MYBex13::TULP4ex2*, *ERCC2* germline mutation
3	69/M	Nasal cavity	Mucoepidermoid carcinoma	Surgery + radiotherapy	NA	NA	*ACTN4ex18::MYBex2*, *MYB* break-apart (FISH), *CHD2*, *TAF1*, *ARID1B*, *RB1*, *APC*, and *CSF3R* mutations
4	82/M	Sphenoid sinus	Adenoid cystic carcinoma	Surgery + radiotherapy	Relapse, progressive disease	DOD or DWD (84)	*EWSR1ex6::MYBex2*, *EWSR1* and *MYB* break-apart (FISH), *PTEN* and *NOTCH3* mutations
5	62/M	Nasal cavity	Adenoid cystic carcinoma	Surgery + radiotherapy+ proton therapy	Residual disease	AWD (103)	*ACTBex3::MYBex3*

AWD indicates alive with disease; DWD, dead with disease; DOD, dead of disease; NA, not available.

including only nonsynonymous variants with coding consequences and read depth > 50, while benign variants according to the ClinVar database[11] were excluded. The remaining subset of variants was checked visually and suspected artefactual variants were excluded.[12]

Fluorescence In Situ Hybridization (FISH) Analysis

Before performing FISH, hematoxylin and eosin-stained slides were examined to determine the areas for cell counting. Then, a 4-μm-thick formalin-fixed, paraffin-embedded section was placed onto a positively charged slide. The unstained slide was routinely deparaffinized and incubated in the 1× Target Retrieval Solution Citrate pH 6 (Dako) for 40 minutes at 95°C, subsequently cooled for 20 minutes at room temperature in the same solution and washed in deionized water for 5 minutes. The slide was digested in protease solution with pepsin (0.5 mg/mL) (Sigma Aldrich) in 0.01 M HCl at 37°C from 45 to 60 minutes according to the sample conditions. The slide was then rinsed in deionized water for 5 minutes, dehydrated in a series of ethanol solutions (70%, 85%, 96% for 2 min each), and air-dried.

The details of *EWSR1*, *MYB*, *NFIB* break-apart, and *MYB*::*NFIB* fusion analysis have been described previously.[13,14] For the detection of *EWSR1*::*MYB* fusion, custom-designed EWSR1::MYB dual fusion probes comprising of catalog 22q12.2. EWSR1 DF 498kb probe and custom MYB probe with chromosomal location: chr6:135,271,382-135,771,382 (Agilent Technologies) were used following similar protocols.

RESULTS

Demographic and Clinicopathological Features

We collected a cohort of 95 cases of AdCC. They were largely characterized by canonical fusions of *MYB::NFIB* (49 cases) and *MYBL1::NFIB* (9 cases) as indicated by NGS and FISH. In an additional 11 cases of AdCC, rearrangements in *MYB* or *NFIB* genes were detected by FISH. In addition, NGS revealed novel noncanonical fusion transcripts, including *EWSR1::MYB*, *ACTB::MYB, ESRRG::DNM3, MYB::TULP4*, and *ACTN4::MYB*, each of them in 1 case.

The clinical features of all 5 cases of AdCC harboring noncanonical gene fusions are summarized in Table 2. The patients were 4 men and 1 woman with an age range from 62 to 87 years (mean, 71 y). For 1 patient, the clinical data were not available. The tumors arose in the nasal cavity (n = 2), the maxillary sinus (n = 1), the sphenoid sinus (n = 1), and the parotid gland (n = 1).

Treatment consisted of excision or radical surgical resection combined with chemotherapy and/or radiation in 3 patients. One patient received only supportive (palliative) care after a diagnostic biopsy. Follow-up data were available for 4/5 patients, and the follow-up period ranged from shortly after diagnosis to 103 months (median, 66 mo). Two patients are alive with the disease, while 2 are dead of the disease at 72 and 84 months after diagnosis, respectively. For the remaining 1 patient, detailed

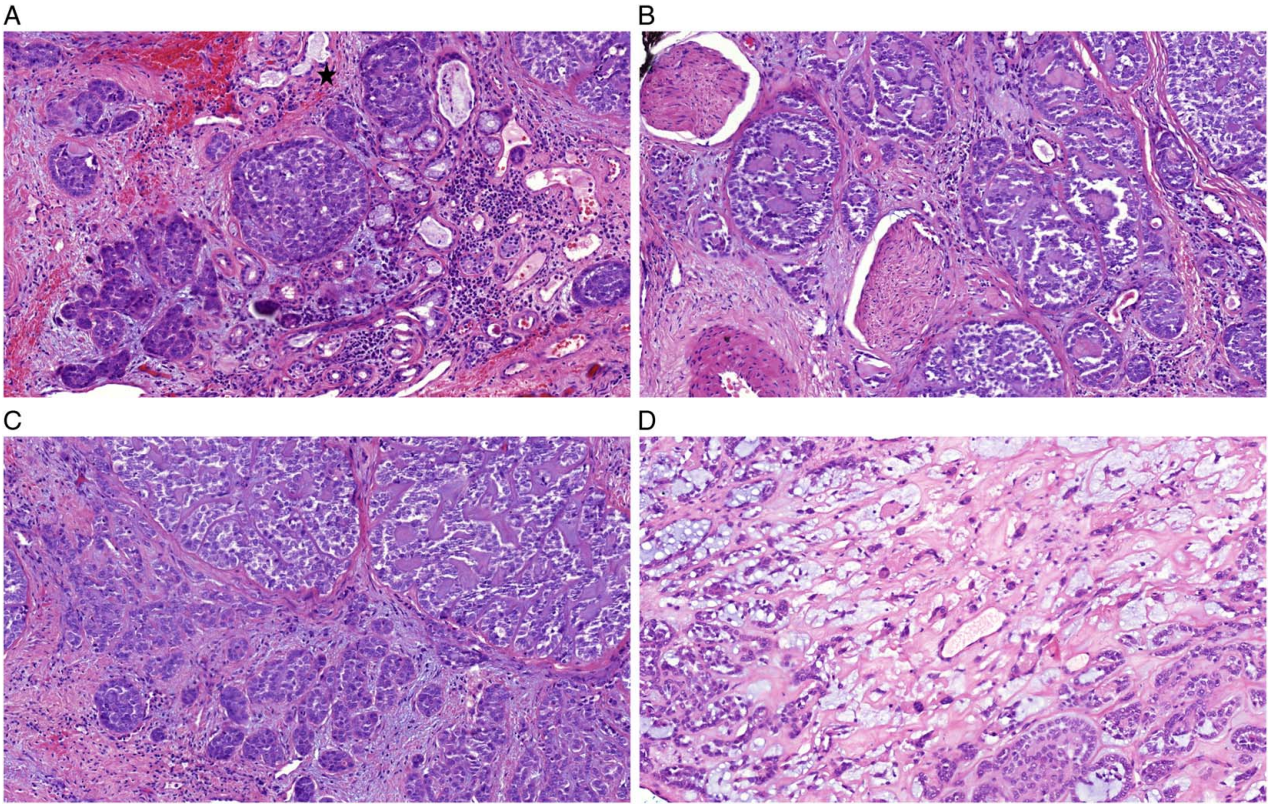

FIGURE 1. In case 1, the tumor consists of areas of the solid growth pattern of adenoid cystic carcinoma with atypical sinonasal glands (*star*) arising from a seromucinous hamartoma (*right side of the picture*) at the periphery of the tumor mass (A). The other growth patterns are cribriform, tubular, and micropapillary (B, C), and there is marked perineural invasion (B). Areas of stromal edema and fibromyxohyaline change are seen in the interstitium, and they contain small clusters or cords of tumor cells, or isolated tumor cells (D).

information regarding therapy and clinical outcome was not available (Table 2).

Histopathologic and Immunohistochemical Finding

Case 1

The patient presented with a polypoid lesion infiltrating the right maxilla. The tumor consisted of a main tumor mass corresponding to AdCC and areas at the periphery of the lesion identical to a seromucinous hamartoma. A transition zone contained atypical sinonasal glands arising from the hamartoma (Fig. 1A) that were connected to the AdCC mass. The AdCC component of the lesion was composed of different architectural patterns, including solid, tubular, micropapillary, and cribriform (containing hyaline or basophilic mucoid material) (Figs. 1B, C). Areas of stromal edema or fibromyxohyaline change of the interstitium were present, and they contained small clusters, cords, or isolated tumor cells (some of them bizarre) (Fig. 1D). The AdCC tumor cells were pleomorphic with irregular nuclear borders, nuclear hyperchromasia, or chromatin clearing with prominent nucleoli and nuclear grooves. The cytoplasm was eosinophilic to clear and bubbly. Perineural invasion was prominent (Fig. 1B). Mitotic activity was high. NGS revealed a unique *ESRRGex3::DNM3ex14* gene fusion of unknown frame and significance, and an *EWSR1* gene break was revealed by FISH.

Case 2

The second case involved an 87-year-old woman who presented with a tumorous growth behind the angle of the mandible since 2 years. The patient recently underwent an exploratory biopsy and is still alive with the disease. The tumor consisted of solid nests of tumor cells that were basophilic and showed peripheral palisading of the nuclei (Fig. 2A). The nuclei were monomorphic with fine chromatin and occasionally with small visible nucleoli. The cytoplasm was watery clear to slightly basophilic, and contained eosinophilic globules in some areas and basement membrane deposits in the center of the tumor nests and also surrounding the tumor cell nests (Fig. 2B). Dense sclerosis was focally present at the edges of the sample (Fig. 2C). No atypical mitoses, necrosis, or invasion were present. Mitotic activity was slightly increased, with the MIB1 index reaching up to 10%. Tumor cells were consistently positive for CK7, SOX10,

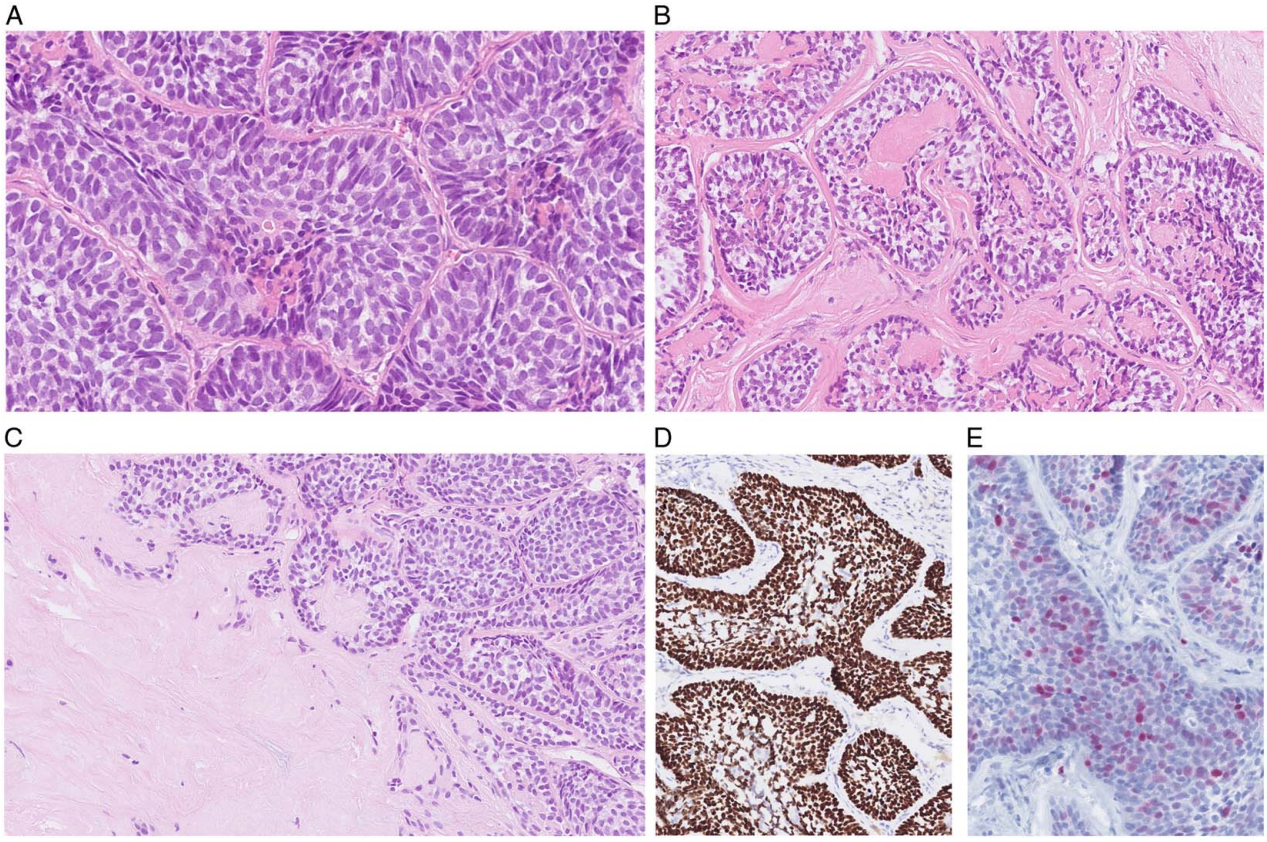

FIGURE 2. Case 2 consists mainly of solid tumor nests with peripheral palisading of the nuclei (A). The tumor cell nests are surrounded by deposits of basement membrane material and eosinophilic globules in the center of the nests and around them (B). Dense sclerosis is present focally at the margins of the specimen (C). Staining for p63 is strongly positive (D). Staining with MYB antibody shows a heterogeneous irregular pattern (E).

and p63 (Fig. 2D). MYB antibody showed irregular nonspecific positivity in 10% of the tumor cells (Fig. 2E). On a diagnostic biopsy, the tumor was signed out as a basocellular neoplasm. Molecular-genetic testing revealed a germline *ERCC2* gene mutation and an in-frame *MYBex13::TULP4ex2* gene fusion. Tumor mutation burden could not be assessed, and microsatellite instability was low (1.83% of loci).

Case 3

In the third case, a 69-year-old man presented with a tumor of the nasal cavity. Microscopically, the tumor consisted of a solidly growing tumor mass composed of 2 populations of cells. The predominant component was composed of monomorphic basaloid cells without significant nuclear atypia and mitotic activity. A less frequent cellular population was represented by groups of cells with pale eosinophilic to vacuolated cytoplasm (Fig. 3A). These cells are identical both in morphology and immunoprofile with cells described by Altemani et al.[15] A stromal component was minor and characterized by mild cellular fibrous bands with distended vascular spaces and large areas of dense sclerosis with mucoid material (Fig. 3B). Basaloid tumor cells were positive for p63 (Fig. 3C) and CK14. Vacuolated (clear) cells showed CK7 expression (Fig. 3D). The Ki-67 proliferation index was estimated at 2%. Molecular genetics revealed an in-frame *ACTN4ex18::MYBex2* gene fusion and a break of the *MYB* gene was shown by FISH. A targeted DNA panel revealed *CHD2 c.4156del p.(Ser1386ValfsTer3)*, *TAF1 c.4882-1G>A*, *ARID1B c.5527C>T, p.(Arg1843Cys)*, *RB1 c.2167dup, p.(Ile723AsnfsTer28)*, *APC c.1213C>T, p.(Arg405Ter)*, and *CSF3R c.1640G>A, p.(Trp547Ter)* pathogenic and likely pathogenic gene mutations. The tumor had a high mutation burden 20.5 mut/Mb) and low microsatellite instability (3.6% of loci).

Case 4

The fourth case was 82-year-old man with a tumor mass of the sphenoid sinus. This case was reported previously.[3] This case is an example of a metatypical AdCC with histologic variability. The tumor was composed of hypercellular and hypocellular areas. The hypercellular areas consisted of basaloid cells forming tubular and cribriform patterns with multiple areas of comedo-like necrosis (Fig. 4A), extensive tubular hypereosinophilia (Fig. 4B), and foci of intraluminal clear cells (Fig. 4C). The islands of tumor cells were

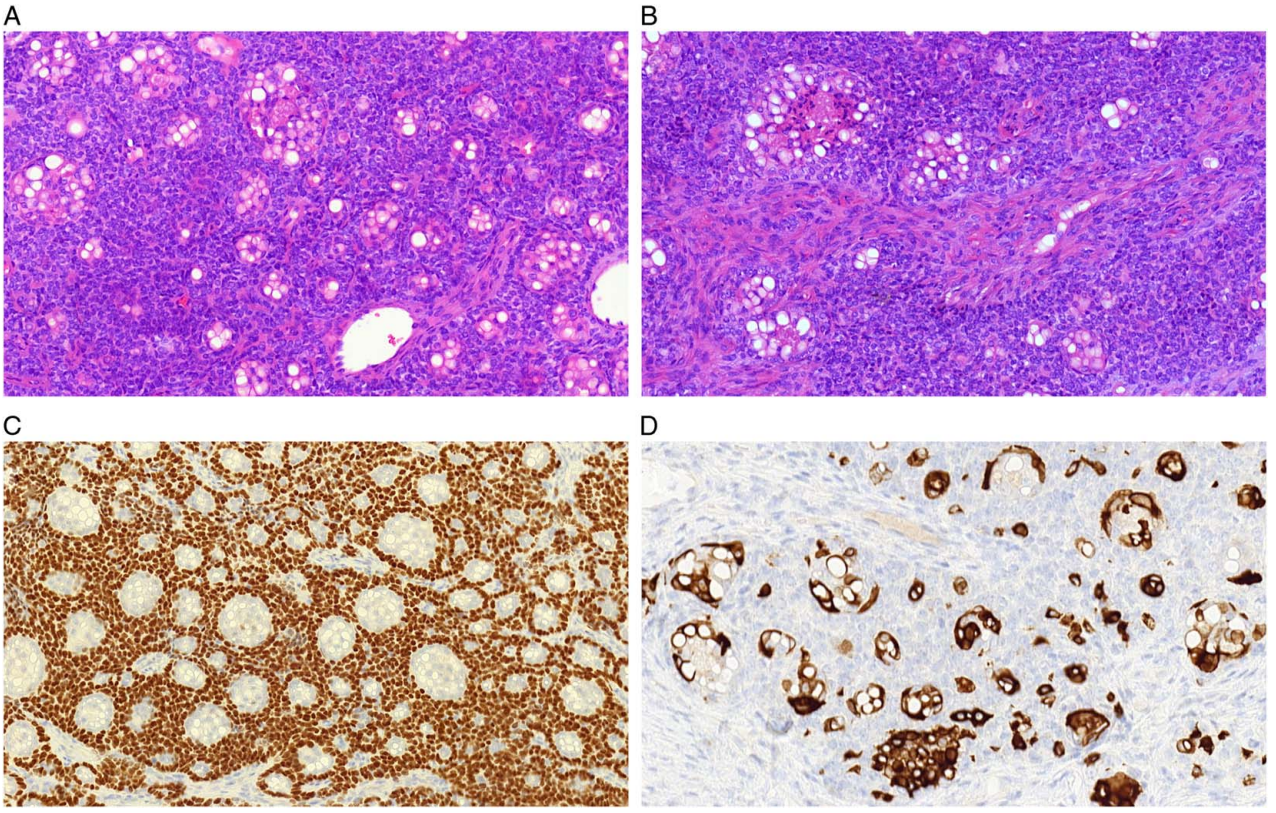

FIGURE 3. Case 3 displays a solid tumor mass composed of a monomorphic population of basaloid cells and groups of cells with pale eosinophilic to vacuolated cytoplasm (A, B). The tumor shows a biphasic immunohistochemical pattern with p63 positivity in the monomorphic cells (C) and CK7 positivity in the vacuolated cells (D).

circumscribed by basement membrane deposits or basophilic mucoid material. The hypocellular area was composed of fibrosclerotic and hyalinized stroma with focal myxoid change and cords and ducts of tumor cells (Figs. 4C, D). Tumor cells were pleomorphic with irregular nuclear borders, nuclear grooves, and multiple nucleoli. The cytoplasm was eosinophilic to clear. Tumor cells showed a typical biphasic immunohistochemical pattern with luminal cells positive for CK7 and abluminal cells positive for p63, CK14, and SOX10. Proliferative activity was intermediate and reached up to 25% in hot spot regions. NGS testing detected an in-frame *EWSR1ex6::MYBex2* gene fusion as well as *PTEN* c.32_33del, p.(Arg11LysfsTer32) and *NOTCH3* c.6692del, p.(Pro2231GlnfsTer15) gene mutations. *EWSR1* and *MYB* breaks were confirmed by FISH.

Case 5

The fifth case concerned a 62-year-old man who underwent an excision of a tumor in the sinonasal tract. The tumor fragments were 8 cm in the largest diameter and macroscopically displayed a mucinous appearance. Microscopic examination revealed a polypoid and partly cystic lesion of predominant myoepithelial appearance with lobulated multinodular architecture, a hypercellular periphery, and hypocellular center with large necrotic areas (Fig. 5A). Tumor cells were basaloid and had monomorphic hyperchromatic nuclei (Fig. 5B). Areas of conventional cribriform adenoid cystic carcinoma were present at the periphery and represented 20% of the tumor mass (Fig. 5C). The stroma was partly hyalinized and partly myxoid. The tumor pattern was biphasic with p63 positivity in cells of the abluminal component (Fig. 5D). The Ki-67 proliferation index was estimated at 30%. Molecular genetics detected an in-frame *ACTBex3::MYBex3* gene fusion. Tumor mutation burden could not be assessed, but microsatellite instability was low (1.96% of loci).

DISCUSSION

Canonical gene fusions have been discovered in 35% to 100% of AdCCs in various studies using reverse transcriptase-polymerase chain reaction and fluorescence in situ hybridization to detect *MYB::NFIB* and/or *MYBL1::NFIB* gene fusions and *MYB*, *NFIB*, and/or *MYBL1* gene breaks, as well as MYB RNA in situ hybridization and NGS platforms.[7,8,10,16,17] Occasional morphologically classic cases of AdCC have been seen that are negative for the above fusions using the aforementioned techniques, either because of insufficient sensitivity of these platforms to identify the fusion or because of alternative molecular changes. The latter could include yet undiscovered fusions, known rare fusions, such as

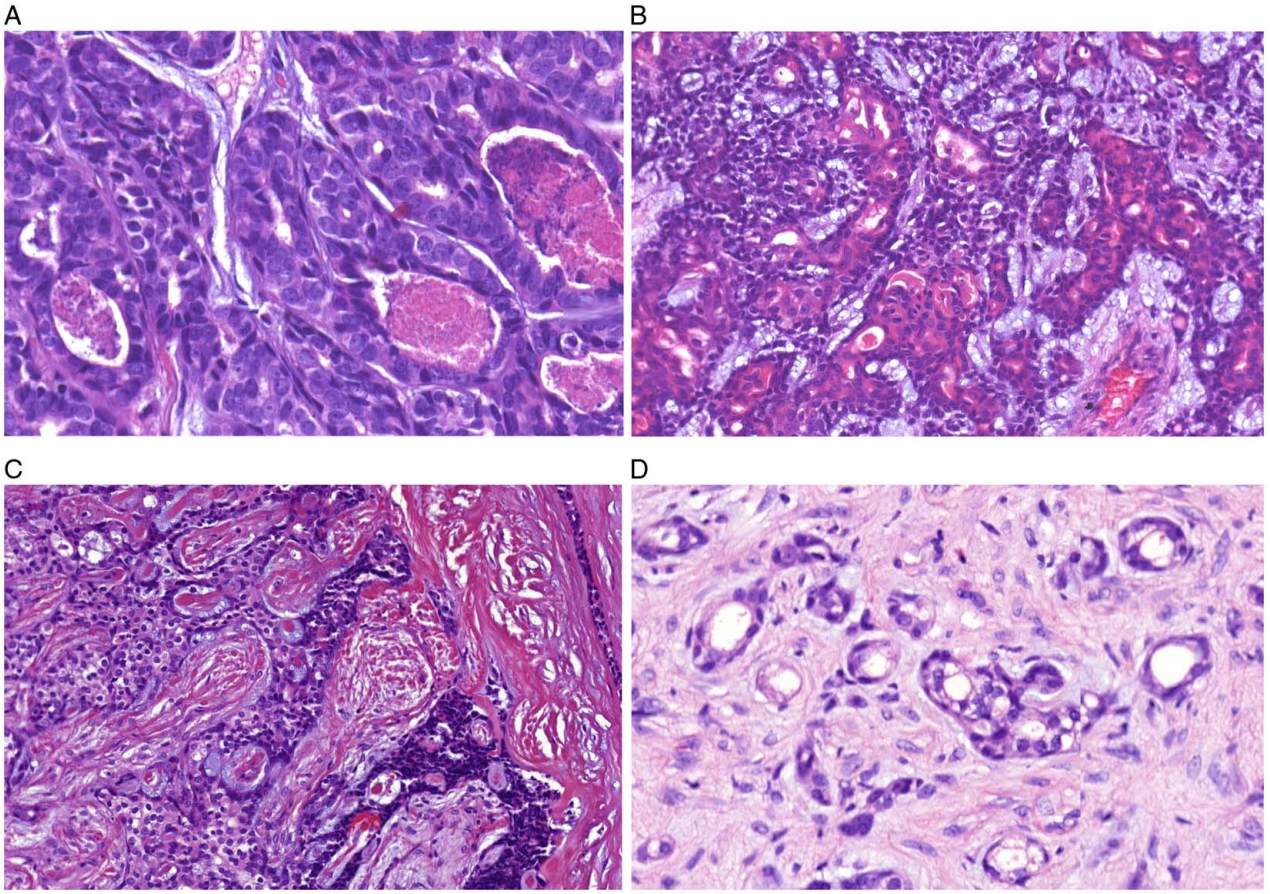

FIGURE 4. The tumor in case 4 displays a hypercellular area with basaloid cells forming tubular and cribriform patterns with multiple areas of comedo-like necrosis (A). Extensive tubular hypereosinophilia (B) and foci of intraluminal clear cells (C) are present in some tumor islands. The tumor cell islands are circumscribed by deposits of basement membrane or basophilic mucoid material (C). A hypocellular area consists of fibrosclerotic and hyalinized stroma with focal myxoid change and cords and ducts of tumor cells (D).

NFIB::AIG1, that are not tested by some targeted panels,[10] or non-fusion events such as *NOTCH* or *TERT* mutations.[18] The fusion status is not thought to be prognostic or significantly associated with any clinicopathologic features, but other mutations might influence treatment options.[18]

Sometimes classic cases of AdCC lack the canonical *MYB*/*MYB1::NFIB* fusions. Thus, even if these genes are included in a targeted gene panel, the canonical fusions cannot be detected in all cases. This may limit our capability as pathologists to quickly provide an accurate diagnosis, especially in the case of biopsies. Therefore, it is important that such samples are then analyzed further in platforms, including genes of the alternative fusions as described in the present study.

Noncanonical fusions of *EWSR1*/*FUS::MYB, MYB::PDCD1LG2,* and *MYB::EFR3A* were previously detected in singular cases in both typical and morphologically unusual AdCC cases of the salivary glands.[9,10] Overall, the canonical and noncanonical fusions lead to overexpression and/or prolongation of the half-life of the rearranged oncogenic Myb transcription factor protein and thus alter the expression of numerous genes involved in cell proliferation, survival, invasiveness, and cell differentiation. The fusion partner of *MYB* may not be necessary for the binding of the fusion protein product to DNA and it might be located at either the 3′ or the 5′ end of the rearranged *MYB* gene. The spectrum of the specific binding sites for the fusion protein product in the genome might, however, be altered in noncanonical fusions.[19–23] The unique morphology of AdCC with alternative noncanonical fusions might, therefore, relate to differential gene expression caused by altered DNA binding activity of these fusion proteins.

In our study, 3 novel fusion partners to *MYB* were detected: *ACTB*, *ACTN4,* and *TULP4*. These discoveries justify further exploration into the intricate molecular mechanisms and their potential implications of this complex spectrum of gene fusions in AdCCs, which have unusual, high-grade, or metatypical morphology. Our cases 1, 3, and 4 displayed morphologic features, including tubular hypereosinophilia, vacuolated clear cells, and

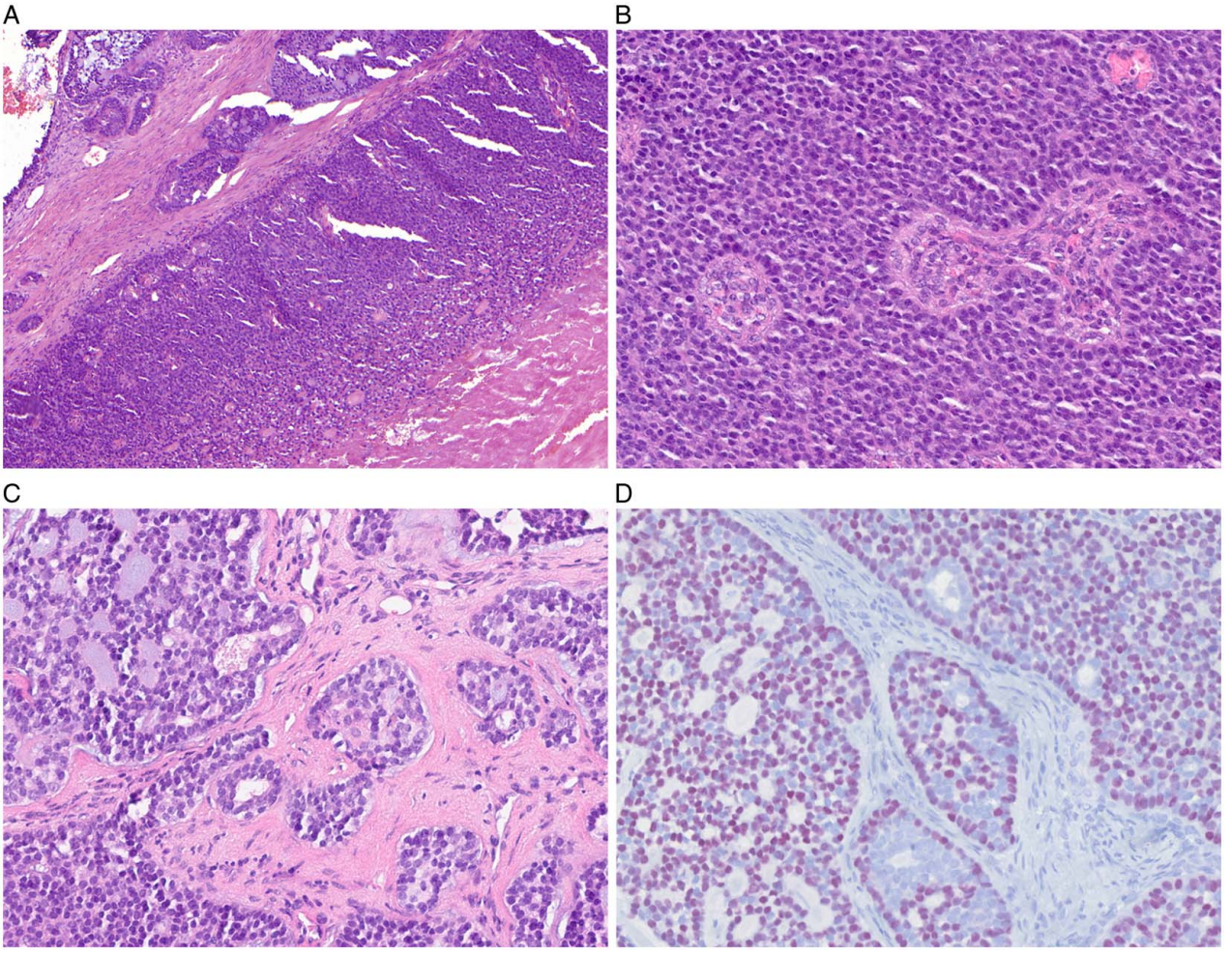

FIGURE 5. In case 5, the tumor is histologically reminiscent of myoepithelial carcinoma with a hypercellular periphery and a hypocellular necrotic center (A). A solid component of the tumor displays circumscribed necrosis and is composed of basaloid cells with monomorphic hyperchromatic nuclei (B). Conventional areas of adenoid cystic carcinoma are localized in the periphery of the lesion (C). Staining for p63 shows nuclear positivity in the abluminal part (D).

small clusters, cords, and isolated tumor cells in the hyalinized extracellular matrix that met criteria of metatypical AdCC[9,24] while cases 2 and 5 showed features of solid atypical morphology. The unusual features of metatypical AdCC were described already by Altemani et al[15] although they did not name the tumor. Their cases have groups of vacuolated neoplastic cells identical to those seen in our case 3.

The *ACTB* gene codes for actin beta, a ubiquitously expressed cytoskeletal protein that is involved in maintaining cell shape, cytoplasmic organization, and integrity. The protein product of the *ACTN4* gene is alpha actinin 4. It is one of the actin-binding proteins that mediates the interaction of actin with cell membranes. The function of the Tulp4 protein has not been well described to date, but it is presumed to be involved in intracellular signaling pathways and was proposed to convey E3 ligase activity.[25]

The *ESRRG::DNM3* fusion was detected in a minor tumor subclone in case 1. Fusions of the *ESRRG* gene have not been reported in English literature to date, while *DNM3* rearrangements are enriched in CNS tissues of ALS patients and in mouse models of breast carcinoma.[26,27] It is an intrachromosomal fusion located on the long arm of chromosome 1. Overall, the significance of this genetic event is unclear and it was presumably not the driver mutation in this case.

While additional mutations in the cases presented herein might modify their morphology or biological behavior, the nucleic acid quality of these consultation cases did not allow for a reliable assessment of mutational status in all cases. However, it should be noted that case 4 harbored *PTEN* and *NOTCH3* deletions and displayed high-grade nuclear features, and these additional genetic events might be associated with tumor progression in this case. Furthermore, case 3 displayed a high number of additional gene mutations, and this was also reflected by a high mutation burden detected by the TS500-targeted NGS panel. These observations suggest that the level of

tumor aggressiveness apparently relates to the number of molecular alterations in the tumor.

CONCLUSIONS

In conclusion, 3 cases of adenoid cystic carcinoma of the salivary glands harbored novel gene fusions not described before: *TULP4::MYB*, *ACTN4::MYB,* and *ACTB::MYB*, each in 1 case. In addition, a rare *EWSR1::MYB* fusion was detected in 1 case. The above noncanonical fusion partners might alter the binding abilities of the altered Myb protein and might, therefore, cause the unusual variant morphologic features seen in these cases. Moreover, 1 case of sinonasal metatypical AdCC with an *EWSR1* rearrangement was detected by FISH and, furthermore, an *ESRRG::DNM3* fusion of unknown significance was described in 1 case.

This study further illustrates the significance of broad molecular profiling in expanding known entities and confirming diagnoses in unusual cases. Drawing conclusions on solely 5 cases is challenging, and a larger study will be necessary to confirm or refute the above hypothesis.

REFERENCES

1. WHO Classification of Tumors Editorial Board. *Head and Neck Tumors*. International Agency for Research on Cancer; 2023 (WHO Classification of Tumors Series, 5th ed.; vol. 9). https://publications.iarc.who.int/629.
2. Skálová A, Hyrcza MD, Vaneček T, et al. Fusion-positive salivary gland carcinomas. *Genes Chromosomes Cancer*. 2022;61:228–243.
3. Skalova A, Vanecek T, Sima R, et al. Mammary analogue secretory carcinoma of salivary glands, containing the *ETV6-NTRK3* fusion gene: a hitherto undescribed salivary gland tumor entity. *Am J Surg Pathol*. 2010;34:599–608.
4. Skalova A, Vanecek T, Martinek P, et al. Molecular profiling of mammary analog secretory carcinoma revealed a subset of tumors harboring a novel *ETV6-RET* translocation: report of 10 cases. *Am J Surg Pathol*. 2018;42:234–246.
5. Rooper L, Karantanos T, Ning Y, et al. Salivary secretory carcinoma with a novel *ETV6-MET* fusion. *Am J Surg Pathol*. 2018;42:1121–1126.
6. Skálová A, Banečkova M, Thompson LDR, et al. Expanding the molecular spectrum of secretory carcinoma of salivary glands with a novel *VIM-RET* fusion. *Am J Surg Pathol*. 2020;44:1295–1307.
7. Mitani Y, Li J, Rao PH, et al. Comprehensive analysis of the *MYB-NFIB* gene fusion in salivary adenoid cystic carcinoma: incidence, variability, and clinicopathologic significance. *Clin Cancer Res*. 2010;16:4722–4731.
8. Mitani Y, Liu B, Rao PH, et al. Novel MYBL1 gene rearrangements with recurrent *MYBL1-NFIB* fusions in salivary adenoid cystic carcinomas lacking t(6;9) translocations. *Clin Cancer Res*. 2016;22:725–733.
9. Weinreb I, Rooper LM, Dickson BC, et al. Adenoid cystic carcinoma with striking tubular hypereosinophilia: a unique pattern associated with nonparotid location and both canonical and novel *EWSR1::MYB* and *FUS::MYB* fusions. *Am J Surg Pathol*. 2023;47:497–503.
10. Mitani Y, Rao PH, Futreal PA, et al. Novel chromosomal rearrangements and break points at the t(6;9) in salivary adenoid cystic carcinoma: association with *MYB-NFIB* chimeric fusion, MYB expression, and clinical outcome. *Clin Cancer Res*. 2011;17:7003–7014.
11. Landrum MJ, Lee JM, Benson M, et al. ClinVar: improving access to variant interpretations and supporting evidence. *Nucleic Acids Res*. 2018;46(D1):D1062–D1067.
12. Koboldt DC. Best practices for variant calling in clinical sequencing. *Genome Med*. 2020;12:91.
13. Šteiner P, Andreasen S, Grossmann P, et al. Prognostic significance of 1p36 locus deletion in adenoid cystic carcinoma of the salivary glands. *Virchows Arch*. 2018;473:471–480.
14. Michal M, Berry RS, Rubin BP, et al. *EWSR1-SMAD3*-rearranged fibroblastic tumor: an emerging entity in an increasingly more complex group of fibroblastic/myofibroblastic neoplasms. *Am J Surg Pathol*. 2018;42:1325–1333.
15. Altemani A, Costa AF, Montalli VA, et al. Signet-ring cell change in adenoid cystic carcinoma: a clinicopathological and immunohistochemical study of four cases. *Histopathology*. 2013;62:531–542.
16. Persson M, Andrén Y, Mark J, et al. Recurrent fusion of MYB and NFIB transcription factor genes in carcinomas of the breast and head and neck. *Proc Natl Acad Sci USA*. 2009;106:18740–18744.
17. Rooper LM, Lombardo KA, Oliai BR, et al. MYB RNA in situ hybridization facilitates sensitive and specific diagnosis of adenoid cystic carcinoma regardless of translocation status. *Am J Surg Pathol*. 2021;45:488–497.
18. Ho AS, Ochoa A, Jayakumaran G, et al. Genetic hallmarks of recurrent/metastatic adenoid cystic carcinoma. *J Clin Invest*. 2019;129:4276–4289.
19. Wagner VP, Bingle CD, Bingle L. MYB-NFIB fusion transcript in adenoid cystic carcinoma: current state of knowledge and future directions. *Crit Rev Oncol Hematol*. 2022;176:103745.
20. Frerich CA, Sedam HN, Kang H, et al. N-terminal truncated Myb with new transcriptional activity produced through use of an alternative MYB promoter in salivary gland adenoid cystic carcinoma. *Cancers (Basel)*. 2019;12:45.
21. Drier Y, Cotton MJ, Williamson KE, et al. An oncogenic MYB feedback loop drives alternate cell fates in adenoid cystic carcinoma. *Nat Genet*. 2016;48:265–272.
22. Gao R, Cao C, Zhang M, et al. A unifying gene signature for adenoid cystic cancer identifies parallel MYB-dependent and MYB-independent therapeutic targets. *Oncotarget*. 2014;5:12528–12542.
23. Corradini F, Cesi V, Bartella V, et al. Enhanced proliferative potential of hematopoietic cells expressing degradation-resistant c-Myb mutants. *J Biol Chem*. 2005;280:30254–30262.
24. Mathew EP, Todorovic E, Truong T, et al. Metatypical adenoid cystic carcinoma: a variant showing prominent squamous differentiation with a predilection for the sinonasal tract and skull base. *Am J Surg Pathol*. 2022;46:816–822.
25. Mukhopadhyay S, Jackson PK. The tubby family proteins. *Genome Biol*. 2011;12:225.
26. Raghav Y, Dilliott AA, Petrozziello T, et al. Identification of gene fusions associated with amyotrophic lateral sclerosis. *Muscle Nerve*. 2024;69:477–489.
27. Liu H, Murphy CJ, Karreth FA, et al. Identifying and targeting sporadic oncogenic genetic aberrations in mouse models of triple-negative breast cancer. *Cancer Discov*. 2018;8:354–369. Erratum in: *Cancer Discov*. 2018 Aug;8(8):1044.

